Three-dimensional helicity distribution functions and EicC projections

中国物理学会高能物理分会第十二届全国会员代表大会暨学术年会

2026 年 7 月 15 日，中国广州

Ke Yang（杨科）

Institute of Frontier and Interdisciplinary Science, Shandong University, Qingdao 266237, China

Transverse Nucleon Tomography Collaboration

Hongxin Dong, Tianbo Liu, Bo-Qiang Ma, Peng Sun,

Chunhua Zeng, Yuxiang Zhao, Yiyu Zhou

Phys. Rev. Lett. 134 (2025) 12, 121902

目录

Introduction

- Protons and neutrons are the primary constituents of visible matter in the universe.

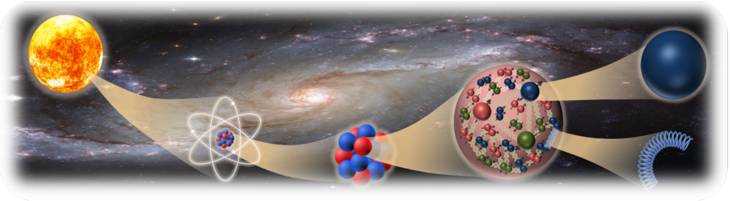

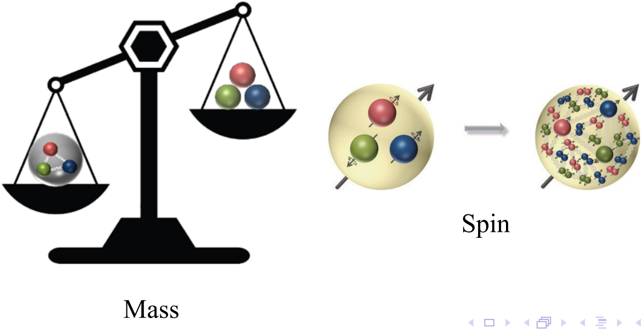

Proton Spin Structure in Naïve Quark Model

M. Gell-Mann, Phys. Lett. 8, 214 (1964);
G. Zweig, CERN Report No. TH-401 (1964).

■ Quark model:

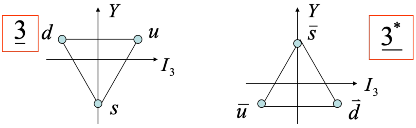

■ Color structure:

$$\underline{3} \times \underline{3}^* = \underline{8} + \boxed{\underline{1}}$$

$$\underline{3} \times \underline{3} \times \underline{3} = \underline{10} + \underline{8} + \underline{8} + \boxed{\underline{1}}$$

■ Proton wave function in spin flavor space:

$$|p_\uparrow\rangle = \frac{1}{\sqrt{18}}\Big[2|u_\uparrow d_\downarrow u_\uparrow\rangle + 2|u_\uparrow u_\uparrow d_\downarrow\rangle + 2|d_\downarrow u_\uparrow u_\uparrow\rangle - |u_\uparrow u_\downarrow d_\uparrow\rangle$$

$$- |u_\uparrow d_\uparrow u_\downarrow\rangle - |u_\downarrow d_\uparrow u_\uparrow\rangle - |d_\uparrow u_\downarrow u_\uparrow\rangle - |d_\uparrow u_\uparrow u_\downarrow\rangle - |u_\downarrow u_\uparrow d_\uparrow\rangle\Big].$$

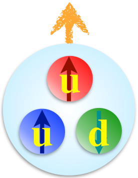

$$\Delta u = u_\uparrow - u_\downarrow = \frac{4}{3}, \qquad \Delta d = d_\uparrow - d_\downarrow = -\frac{1}{3}$$

The spin of the proton comes entirely from the spin of the quarks!

Proton Spin Structure

J. Ashman et al. (EMC) PLB 206, 364 (1988).

J. Ashman et al. (EMC) NP B328, 1 (1989).

■ Experimental data:

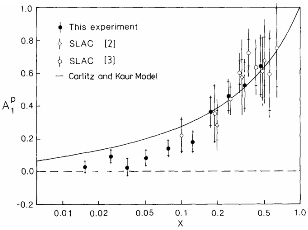

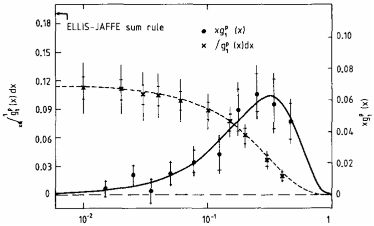

$$\Delta\Sigma = 0.114 \pm 0.012 \pm 0.026$$

$$\Delta\Sigma = 0.126 \pm 0.010 \pm 0.015$$

■ Global analysis:

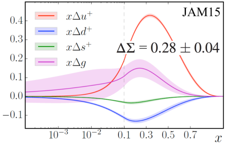

JAM Collaboration, PR D 93, 074005 (2016).

$$\Delta\Sigma = 0.28 \pm 0.04$$

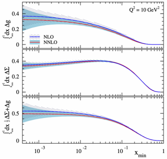

I. Borsa et al. Phys.Rev.Lett. 133, 151901 (2024).

$$\Delta\Sigma \sim 0.35$$

■ Lattice calculation:

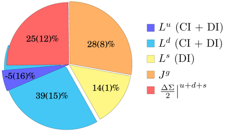

χQCD Collaboration, PR D 91, 014505 (2015).

$$\Delta\Sigma \sim 0.25 \pm 0.12$$

Proton Spin Structure

■ Spin decomposition:

R. Jaffe and A. Manohar, Nucl.Phys. B337 (1990) 509.

$$J = \frac{1}{2}\Delta\Sigma + L_q + \Delta G + L_g,$$

$$\Delta\Sigma = \Delta u + \Delta d \sim 0.3$$

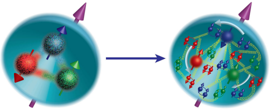

■ Melosh-Wigner rotation: nucleon in its rest frame V.S. in infinite momentum frame

E. P. Wigner, Annals Math. 40, 149 (1939);H. J. Melosh, Phys. Rev. D 9, 1095 (1974).

spin state

$$\chi_T^{\uparrow} = w\left[(k^+ + m)\chi_F^{\uparrow} - (k^1 + ik^2)\chi_F^{\downarrow}\right] \qquad k^+ = k^0 + k^3$$

$$\chi_T^{\downarrow} = w\left[(k^+ + m)\chi_F^{\downarrow} + (k^1 - ik^2)\chi_F^{\uparrow}\right] \qquad w = \left[2k^+(k^0 + m)\right]^{-1/2}$$

Quark polarization state

$$\Delta q = \int d^3\mathbf{k}\,\mathcal{M}\left[q^{\uparrow}(k) - q^{\downarrow}(k)\right] \qquad \mathcal{M} = \frac{(k^+ + m)^2 - k_T^2}{2k^+(k^0 + m)}$$

B.-Q. Ma, J. Phys. G 17, L53-L58 (1991);B.-Q. Ma, Z.Phys. C 58, 479 (1993).

The Melosh-Wigner rotation predicts decreasing polarization with transverse momentum, and this prediction should be tested by data.

Transverse Momentum Dependent PDFs

■ Definition

R. Boussarie, et al. TMD Handbook, arXiv:2304.03302.

$$\Phi_{ij}(x,p_T) = \int \frac{\mathrm{d}\xi^- \mathrm{d}^2\xi_T}{(2\pi)^3}\, e^{ip\cdot\xi} \langle P|\bar{\psi}_j(0)\, \mathcal{U}^{n^-}_{(0,+\infty)}\, \mathcal{U}^{n^-}_{(+\infty,\xi)}\, \psi_i(\xi)|P\rangle\Big|_{\xi^+=0}$$

Nucleon Polarization	Quark Polarization: Un-Polarized (U)	Quark Polarization: Longitudinally Polarized (L)	Quark Polarization: Transversely Polarized (T)
U	f_1 = Unpolarized		$h_1^\perp$ = − Boer-Mulders
L		g_1 = − Helicity	$h_{1L}^\perp$ = − Worm-gear
T	$f_{1T}^\perp$ = − Sivers	$g_{1T}^\perp$ = − Worm-gear	h_1 = − Transversity $h_{1T}^\perp$ = − Pretzelosity

Structure functions of SIDIS

- **SIDIS process:** $\ell(l) + N(P) \to \ell(l') + h(P_h) + X$

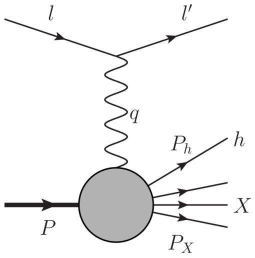

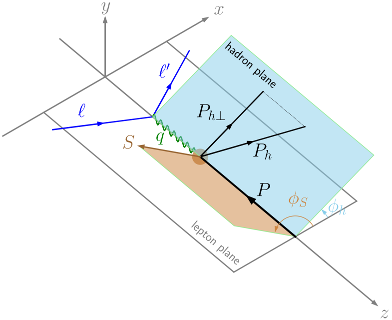

$$q^2 = -Q^2, \qquad x = \frac{Q^2}{2P\cdot q}, \qquad y = \frac{P\cdot q}{P\cdot l}$$

$$z = \frac{P\cdot P_h}{P\cdot q}, \qquad \gamma = \frac{2M_N x}{Q}, \qquad \epsilon = \frac{1-y-\frac{1}{4}\gamma^2y^2}{1-y+\frac{1}{2}y^2+\frac{1}{4}\gamma^2y^2}$$

$$\cos\phi_h = -\frac{l_\mu P_{h\nu} g_\perp^{\mu\nu}}{l_\perp P_{hT}}, \qquad \cos\phi_S = -\frac{l_\mu S_{\perp\nu} g_\perp^{\mu\nu}}{l_\perp S_\perp},$$

$$\sin\phi_h = -\frac{l_\mu P_{h\nu} \epsilon_\perp^{\mu\nu}}{l_\perp P_{hT}}, \qquad \sin\phi_S = -\frac{l_\mu S_{\perp\nu} \epsilon_\perp^{\mu\nu}}{l_\perp S_\perp},$$

Trento convention

Structure functions of SIDIS

$$
\begin{aligned}
&\frac{d\sigma}{dx\,dy\,dz\,dP_{hT}^2\,d\phi_h\,d\phi_S} \\
&= \frac{\alpha^2}{xyQ^2}\,\frac{y^2}{2(1-\epsilon)}\left(1+\frac{\gamma^2}{2x}\right)\times\Big\{ \\
&\quad F_{UU,T}+\epsilon F_{UU,L}+\sqrt{2\epsilon(1+\epsilon)}F_{UU}^{\cos\phi_h}\cos\phi_h \\
&\quad +\epsilon F_{UU}^{\cos 2\phi_h}\cos 2\phi_h+\lambda_e\sqrt{2\epsilon(1-\epsilon)}F_{LU}^{\sin\phi_h}\sin\phi_h \\
&\quad +S_L\Big[\sqrt{2\epsilon(1+\epsilon)}F_{UL}^{\sin\phi_h}\sin\phi_h+\epsilon F_{UL}^{\sin 2\phi_h}\sin 2\phi_h\Big] \\
&\quad +\lambda_e S_L\Big[\sqrt{1-\epsilon^2}F_{LL}+\sqrt{2\epsilon(1-\epsilon)}F_{LL}^{\cos\phi_h}\cos\phi_h\Big] \\
&\quad +S_T\Big[\Big(F_{UT,T}^{\sin(\phi_h-\phi_S)}+\epsilon F_{UT,L}^{\sin(\phi_h-\phi_S)}\Big)\sin(\phi_h-\phi_S) \\
&\qquad +\epsilon F_{UT}^{\sin(\phi_h+\phi_S)}\sin(\phi_h+\phi_S)+\epsilon F_{UT}^{\sin(3\phi_h-\phi_S)}\sin(3\phi_h-\phi_S) \\
&\qquad +\sqrt{2\epsilon(1+\epsilon)}F_{UT}^{\sin\phi_S}\sin\phi_S+\sqrt{2\epsilon(1+\epsilon)}F_{UT}^{\sin(2\phi_h-\phi_S)}\sin(2\phi_h-\phi_S)\Big] \\
&\quad +\lambda_e S_T\Big[\sqrt{1-\epsilon^2}F_{LT}^{\cos(\phi_h-\phi_S)}\cos(\phi_h-\phi_S) \\
&\qquad +\sqrt{2\epsilon(1-\epsilon)}F_{LT}^{\cos\phi_S}\cos\phi_S+\sqrt{2\epsilon(1-\epsilon)}F_{LT}^{\cos(2\phi_h-\phi_S)}\cos(2\phi_h-\phi_S)\Big]\Big\}
\end{aligned}
$$

A. Bacchetta, J. High Energy Phys. 02 (2007) 093.

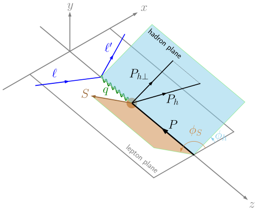

$$F_{AB,C}^{m}(x,z,P_{hT}^2,Q^2)\sim f\otimes D$$

- A : lepton polarization
- B : nucleon polarization
- C : virtual photon polarization
- m : angular modulation

18 structure functions.

Double Spin Asymmetry

■ **Asymmetry from cross section to structure functions:**

$$A_{LL}(\phi_h) = \frac{1}{|S_\perp||\lambda_e|}\frac{[\mathrm{d}\sigma_{LL}(+,+) - \mathrm{d}\sigma_{LL}(-,+)]}{\mathrm{d}\sigma_{LL}(+,+) + \mathrm{d}\sigma_{LL}(-,+)}$$
$$= \sqrt{1-\varepsilon^2}\,\frac{F_{LL}}{F_{UU,T}} + \sqrt{2\varepsilon(1-\varepsilon)}\cos\phi_h \frac{F_{LL}^{\cos\phi_h}}{F_{UU,T}}.$$

$$A_{LL} = \sqrt{1-\varepsilon^2}\,\frac{F_{LL}}{F_{UU,T}}$$
$$A_{LL}^{\cos\phi_h} = \sqrt{2\varepsilon(1-\varepsilon)}\,\frac{F_{LL}^{\cos\phi_h}}{F_{UU,T}}$$

■ **Structure functions as TMD convolutions:**

$$F_{UU,T} = \mathcal{C}[f_1 D_1], \qquad F_{LL} = \mathcal{C}[g_{1L} D_1],$$
$$x g_L^\perp = x\tilde{g}_L^\perp + g_{1L} + \frac{m}{M_N} h_{1L}^\perp \approx g_{1L}.$$
$$F_{LL}^{\cos\phi} = \frac{2M}{Q}\mathcal{C}\Big[\frac{\hat{\mathbf{h}}\cdot\mathbf{p}_T}{M_h}\Big(x e_L H_1^\perp - \frac{M_h}{M} g_{1L}\frac{\tilde{D}^\perp}{z}\Big)$$
$$- \frac{\hat{\mathbf{h}}\cdot\mathbf{k}_T}{M}\Big(x g_L^\perp D_1 + \frac{M_h}{M} h_{1L}^\perp \frac{\tilde{E}}{z}\Big)\Big]$$
$$\approx -\frac{2M}{Q}\mathcal{C}\left[\frac{\hat{\mathbf{h}}\cdot\mathbf{k}_T}{M}(g_{1L} D_1)\right]$$

TMD PDF

$f_1(x, k_T)$

$g_{1L}(x, k_T)$

TMD FF

$D_1(x, p_T)$

Energy Evolution

R. Boussarie, et al. TMD Handbook, arXiv:2304.03302.

■ double scale evolution:

$$\mu \frac{\mathrm{d}\mathcal{F}(x,b_T;\mu,\zeta)}{\mathrm{d}\mu} = \gamma_\mu(\mu,\zeta)\mathcal{F}(x,b_T;\mu,\zeta)$$

$$\zeta \frac{\mathrm{d}\mathcal{F}(x,b_T;\mu,\zeta)}{\mathrm{d}\zeta} = -\mathcal{D}(\mu,b_T)\mathcal{F}(x,b_T;\mu,\zeta)$$

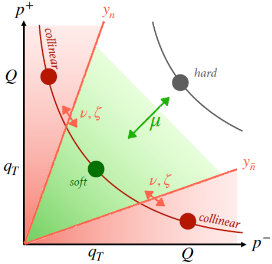

■ ζ-prescription evolution path:

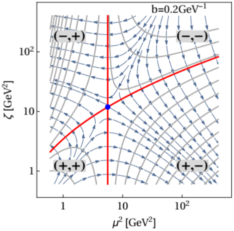

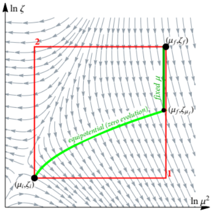

$$R[b_T;(\mu_i,\zeta_i)\to(Q,Q^2)] = \left[\frac{Q^2}{\zeta_\mu(Q,b_T)}\right]^{-\mathcal{D}(Q,b_T)}$$

I. Scimemi and A. Vladimirov, J. High Energy Phys. 06 (2020) 137.

World SIDIS Data

Data set	Run	Target	Beam	N_{tot} (cut)	Process
HERMES	1996–2000	H_2	27.6 GeV $e^\pm$	80(42)	$e^\pm p \to e^\pm \pi^+ X$
HERMES	1996–2000	H_2	27.6 GeV $e^\pm$	80(42)	$e^\pm p \to e^\pm \pi^- X$
HERMES	1996–2000	D_2	27.6 GeV $e^\pm$	80(39)	$e^\pm d \to e^\pm \pi^+ X$
HERMES	1996–2000	D_2	27.6 GeV $e^\pm$	80(37)	$e^\pm d \to e^\pm \pi^- X$
HERMES	1996–2000	D_2	27.6 GeV $e^\pm$	79(40)	$e^\pm d \to e^\pm K^+ X$
HERMES	1996–2000	D_2	27.6 GeV $e^\pm$	80(38)	$e^\pm d \to e^\pm K^- X$
CLAS	2009	$^{14}NH_3$	6 GeV e^-	21(8)	$e^- p \to e^- \pi^0 X$
Total				498(246)	

HERMES, Phys. Rev. D 99, 112001 (2019). CLAS, Phys. Lett. B 782, 662 (2018).

To be consistent with the TMD factorization framework, we apply a data cut: $q_T/Q < 0.5$. Numbers in parentheses indicate the remaining data points after the cut. After the cut, 246 data points remain.

The Electron-Ion Collider in China

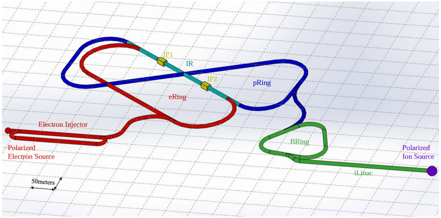

Table 1.1: Available particles and their corresponding energy, polarization, luminosity and integrated luminosity.

Particle	Momentum (GeV/c/u)	CM energy (GeV/u)	Average Polarization	Luminosity at the nucleon level ($cm^{-2}s^{-1}$)	Integrated luminosity (fb^{-1})
e	3.5		80%		
p	20	16.76	70%	2.00×10^{33}	50.5
d	12.90	13.48	Yes	8.48×10^{32}	21.4
$^{3}He^{++}$	17.21	15.55	Yes	6.29×10^{32}	15.9
$^{7}Li^{3+}$	11.05	12.48	No	9.75×10^{32}	24.6
$^{12}C^{6+}$	12.90	13.48	No	8.35×10^{32}	21.1
$^{40}Ca^{20+}$	12.90	13.48	No	8.35×10^{32}	21.1
$^{197}Au^{79+}$	10.35	12.09	No	9.37×10^{32}	23.6
$^{208}Pb^{82+}$	10.17	11.98	No	9.22×10^{32}	23.3
$^{238}U^{92+}$	9.98	11.87	No	8.92×10^{32}	22.5

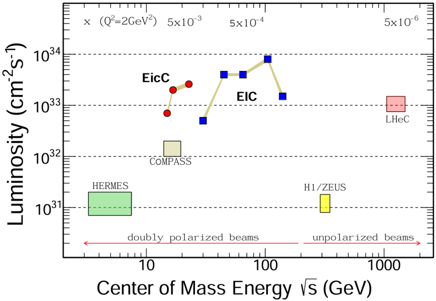

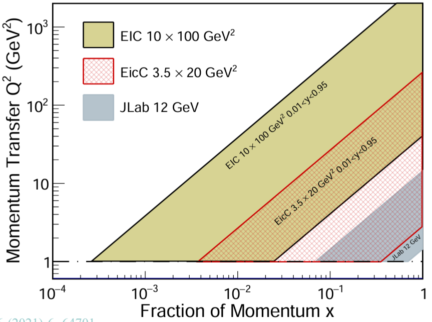

D. P. Anderle et al. Front.Phys.(Beijing) 16 (2021) 6, 64701.

Data Kinematic Distributions

■ **World data kinematic coverage:**

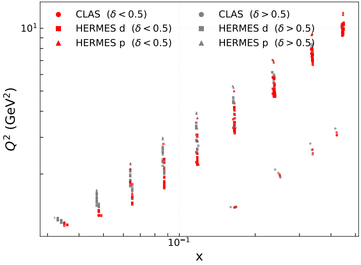

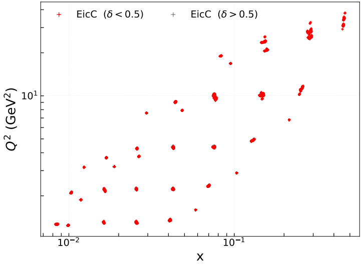

The world data cover relatively low Q^2 region, and therefore we incorporate target mass corrections.

$$x_S = \frac{2x}{\gamma^2}\left[\sqrt{1+\gamma^2\left(1-\frac{\mathbf{q}_T^2}{Q^2}\right)}-1\right]. \qquad z_S = z\,\frac{x_S}{x}\,\frac{1+\sqrt{1-\varsigma_h^2}}{2\left(1-\frac{\mathbf{q}_T^2}{Q^2}\right)}.$$

$$\mathbf{q}_T = -\frac{\mathbf{P}_{hT}}{z}\sqrt{\frac{1+\gamma^2}{1-\varsigma_h^2}}. \qquad \varsigma_h^2 \equiv \frac{4x^2M^2m_h^2}{z^2Q^4} = \gamma^2\,\frac{m_h^2}{z^2Q^2}.$$

Parametrization

■ Parametrization of $g_{1L}(x, b_T)$ at saddle point:

$$g_{1L}^{f}(x,b_T)=\sum_{f'}\int_x^1\frac{\mathrm{d}\xi}{\xi}\Delta C_{f\leftarrow f'}(\xi,b_T,\mu_{\mathrm{OPE}})\times g_{1L}^{f'}\left(\frac{x}{\xi},\mu_{\mathrm{OPE}}\right)g_{\mathrm{NP}}(x,b_T).$$

Modified collinear helicity distribution input, with α, β, ε as free parameters to be fitted:

$$g_{1L}^{f}(x,\mu_{\mathrm{OPE}})=N_f\frac{(1-x)^{\alpha_f}x^{\beta_f}(1+\varepsilon_f x)}{n(\alpha_f,\beta_f,\varepsilon_f)}g_1^f(x,\mu_{\mathrm{OPE}})$$

The x-shape modification can be removed by setting $\alpha, \beta, \varepsilon = 0$. g_1 is the collinear helicity distribution input. The $n(\alpha, \beta, \varepsilon)$ factor is introduced to decouple the normalization from the shape parameters. The non-perturbative function is parametrized as

$$g_{\mathrm{NP}}(x,b_T)=\exp\left[-(\lambda_1(1-x)+\lambda_2 x+x(1-x)\lambda_5)b_T^2\right]$$

■ TMD helicity distribution at final energy scale:

$$g_{1L}(x,b_T;Q,Q^2)=R(b_T,Q)g_{1L}(x,b_T)$$

Numerical Method

■ **world data fit:**

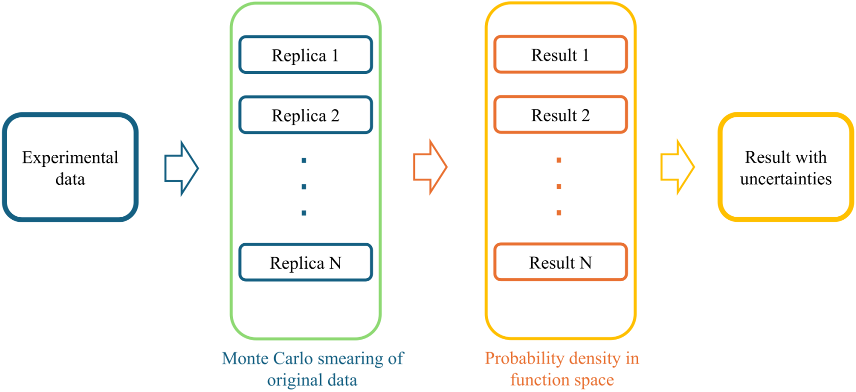

To remove the systematic underestimation caused by the D'Agostini bias, we performed T0-prescription iteration.

■ **EicC projection:** We used the world data fit results to make projections for EicC, and then added the projected EicC data into the data list and refitted.

Results

■ Extracted three-dimensional helicity distribution functions

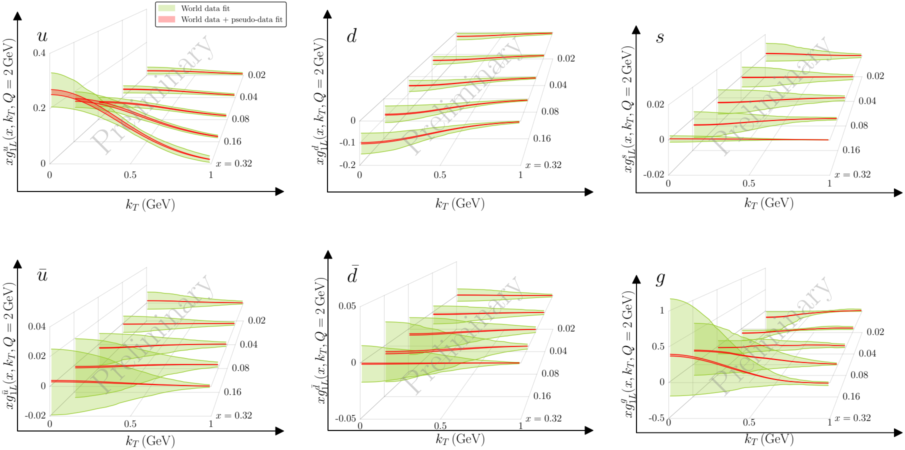

Results

■ Polarization of up quark and down quark

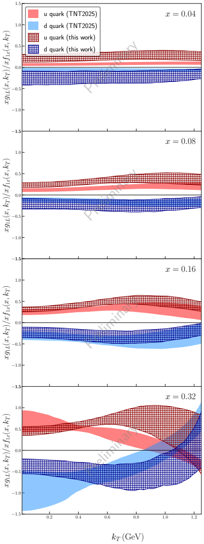

$$g_{1L}(x,k_T^2) = q_{\uparrow}(x,k_T^2) - q_{\downarrow}(x,k_T^2)$$

quantifies the net density difference between quarks with spin parallel and antiparallel to the spin of a polarized proton.

$$\frac{g_{1L}(x,k_T^2)}{f_1(x,k_T^2)} = \frac{q_{\uparrow}(x,k_T^2) - q_{\downarrow}(x,k_T^2)}{q_{\uparrow}(x,k_T^2) + q_{\downarrow}(x,k_T^2)}$$

quantifies the polarization rate of quarks.

In the intermediate x region where valence quarks dominate, the polarization is most pronounced at small k_T and falls off with increasing transverse momentum, consistent with the prediction of the Melosh-Wigner rotation effect.

Results

■ Polarization of up quark and down quark

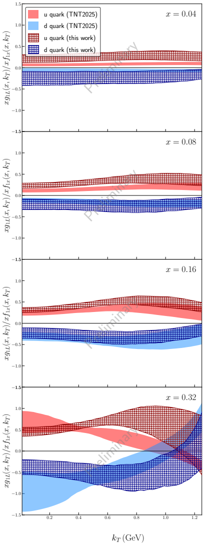

MAP, Phys.Rev.Lett. 134, 12, 121901 (2025).

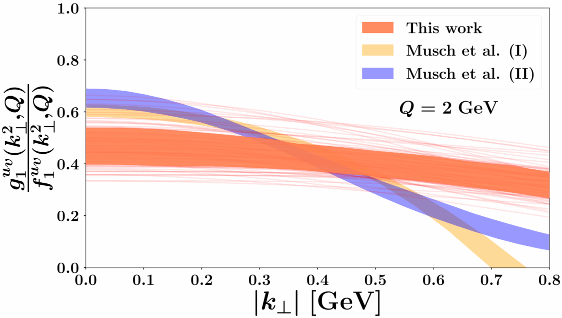

Results

Polarization of up quark and down quark

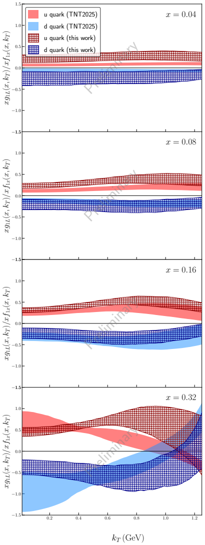

$$g_{1L}(x, k_T^2) = q_\uparrow(x, k_T^2) - q_\downarrow(x, k_T^2)$$

quantifies the net density difference between quarks with spin parallel and antiparallel to the spin of a polarized proton.

$$\frac{g_{1L}(x, k_T^2)}{f_1(x, k_T^2)} = \frac{q_\uparrow(x, k_T^2) - q_\downarrow(x, k_T^2)}{q_\uparrow(x, k_T^2) + q_\downarrow(x, k_T^2)}$$

quantifies the polarization rate of quarks.

At lower x, where sea quarks and gluons dominate, the trend of polarization with k_T is not obvious, implying rich underlying QCD dynamics.

Result

■ Impact from EicC pseudo-data

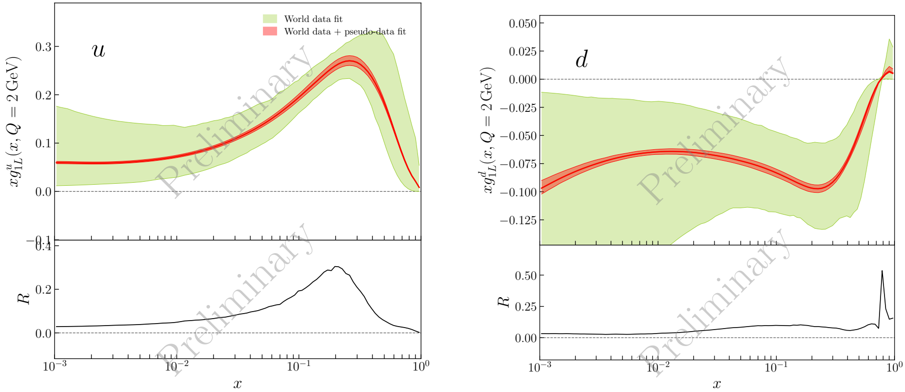

The proposed EicC will enhance the precision of helicity distribution especially for $x > 10^{-3}$.

Result

■ Consistency with collinear helicity distribution functions

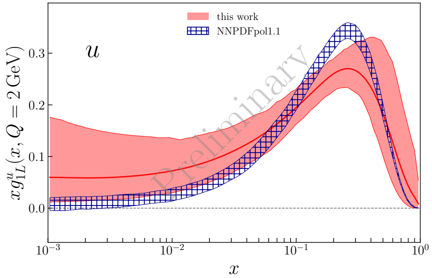

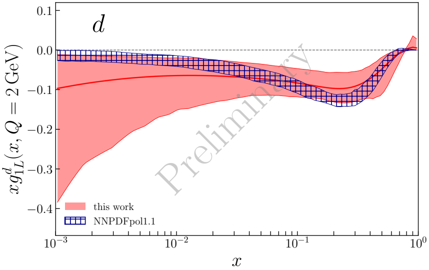

Summary

Summary

- We updated the extraction of three-dimensional helicity distributions, incorporating mass corrections and improving the small-b_T matching to NNLO.
- The extracted u and d quark helicity distribution functions are consistent with collinear results. For sea quarks, current data do not yet provide strong constraints.
- In the valence quark region, polarization is concentrated at small k_T, consistent with the Melosh-Wigner rotation prediction, while the trend at small x is not obvious, likely reflecting QCD dynamical effects.
- We performed EicC projection studies and find that the anticipated EicC data can significantly improve the precision of three-dimensional helicity distribution extraction.

Thanks

Some tables

Parameter	Value	Parameter	Value
χ^2	$491.0^{+77.85}_{-71.57}$	calls	2875^{+1270}_{-1077}
N_u	$0.05283^{+0.05795}_{-0.02016}$	N_d	$0.05220^{+0.07332}_{-0.03045}$
N_s	$-0.001711^{+0.06575}_{-0.05296}$	$N_{\bar{u}}$	$0.02560^{+0.1895}_{-0.2135}$
$N_{\bar{d}}$	$0.007628^{+0.08353}_{-0.08332}$	N_g	$0.09830^{+0.1246}_{-0.1323}$
α_u	$-1.781^{+1.341}_{-1.219}$	β_u	$-0.4275^{+0.3021}_{-0.3428}$
ϵ_u	$-0.3905^{+1.412}_{-0.3562}$	$\lambda_{1,u}$	$0.1431^{+0.08415}_{-0.08316}$
$\lambda_{2,u}$	$0.6072^{+1.168}_{-0.6072}$	$\lambda_{5,u}$	$-1.057^{+1.134}_{-1.692}$
$\lambda_{5,u}$	$0.2341^{+0.1574}_{-0.2295}$	r_{CLAS}	$-0.03810^{+0.4509}_{-0.5222}$
$r_{HERMES,p}$	$-0.3676^{+0.4145}_{-0.4357}$	$r_{HERMES,d}$	$0.3828^{+0.2086}_{-0.2306}$

Parameter	Value
$\chi^2_{\mathrm{CLAS}}\vert pt$	0.5572
$\chi^2_{\mathrm{HERMESp}}\vert pt$	0.7543
$\chi^2_{\mathrm{HERMESd}}\vert pt$	0.7862
$\chi^2_{\mathrm{total}}\vert pt$	0.7675

Some tables

Collaboration	Run	Process	Polarization	Dilution
HERMES	1996–2000	$e^{\pm}p \to e^{\pm}hX$	6.6%	0
HERMES	1996–2000	$e^{\pm}d \to e^{\pm}hX$	5.7%	0
CLAS	2009	$e^{-}p \to e^{-}\pi^{0}X$	4.5% = 2% + 4%	5.8% = 3% + 5%
EicC	proposed	$e^{-}p \to e^{-}\pi^{+}X$	$2\% + 3\%$	0
EicC	proposed	$e^{-}p \to e^{-}\pi^{-}X$	$2\% + 3\%$	0
EicC	proposed	$e^{-}p \to e^{-}K^{+}X$	$2\% + 3\%$	0
EicC	proposed	$e^{-}p \to e^{-}K^{-}X$	$2\% + 3\%$	0
EicC	proposed	$e^{-}n \to e^{-}\pi^{+}X$	$2\% + 3\% + 4\%$	0
EicC	proposed	$e^{-}n \to e^{-}\pi^{-}X$	$2\% + 3\% + 4\%$	0
EicC	proposed	$e^{-}n \to e^{-}K^{+}X$	$2\% + 3\% + 4\%$	0
EicC	proposed	$e^{-}n \to e^{-}K^{-}X$	$2\% + 3\% + 4\%$	0

R	Γ_{cusp} α_s^3	γ_V α_s^2	$\mathcal{D}_{\mathrm{resum}}$ α_s^2	$\zeta_\mu^{\mathrm{pert}}$ α_s^1	$\zeta_\mu^{\mathrm{exact}}$ α_s^1
$C(\mathbb{C})$	f_1 $\alpha_s^1 \to \alpha_s^2$	D_1 $\alpha_s^1 \to \alpha_s^2$	g_{1L} $\alpha_s^1 \to \alpha_s^2$		

parameters correlation

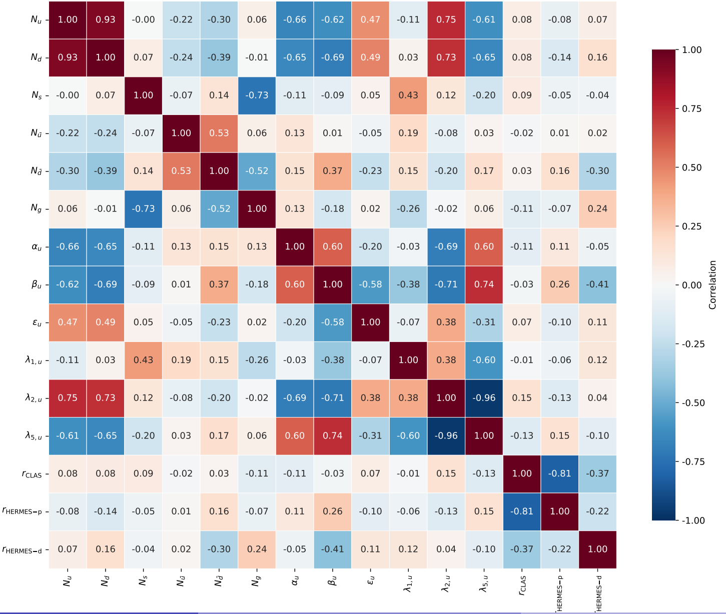

Positivity Bound: Toy Model Test

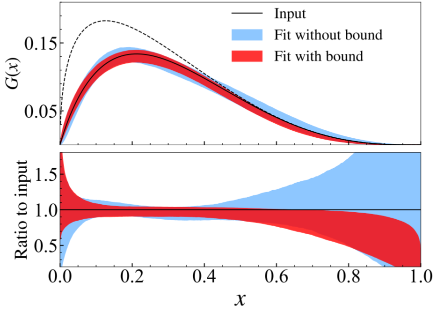

Toy model set:

$$F(x) = x^{0.5}(1-x)^3(1-\sqrt{x}+x),$$

$$G(x) = 2x(1-x)^3(1-\sqrt{x}+0.5x),$$

$$G(x) < F(x)$$

We generate asymmetry $G(x)/F(x)$ in 15 bins as pseudo-data, with a background disturbance $B(x)$. We compare the extracted $G(x)$ from the pseudo-data with and without the application of the positivity constraint.

It was found that imposing the bound during the fitting procedure introduced a bias.